Inorganic Chemistry
Article

Inorg. Chem. **2010**, *49*, 11133–11141 **11133**
DOI: 10.1021/ic101709q

Reactivity of Bis(2,2,5,5-tetramethyl-2,5-disila-1-azacyclopent-1-yl)tin with CO_2, OCS, and CS_2 and Comparison to That of Bis[bis(trimethylsilyl)amido]tin

Constantine A. Stewart,[†] Diane A. Dickie,[‡] Marie V. Parkes,[‡] Josephat A. Saria,[‡] and Richard A. Kemp*[,†,‡]

[†]*Advanced Materials Laboratory, Sandia National Laboratories, Albuquerque, New Mexico 87106, United States, and* [‡]*Department of Chemistry and Chemical Biology, University of New Mexico, Albuquerque, New Mexico 87131, United States*

Received August 23, 2010

The heterocumulenes carbon dioxide (CO_2), carbonyl sulfide (OCS), and carbon disulfide (CS_2) were treated with bis(2,2,5,5-tetramethyl-2,5-disila-1-azacyclopent-1-yl)tin $\{[(CH_2)Me_2Si]_2N\}_2Sn$, an analogue of the well-studied bis[bis(trimethylsilyl)amido]tin species $[(Me_3Si)_2N]_2Sn$, to yield an unexpectedly diverse product slate. Reaction of $\{[(CH_2)Me_2Si]_2N\}_2Sn$ with CO_2 resulted in the formation of 2,2,5,5-tetramethyl-2,5-disila-1-oxacyclopentane, along with $Sn_4(\mu_4\text{-}O)\{\mu_2\text{-}O_2CN[SiMe_2(CH_2)_2]\}_4(\mu_2\text{-}N{=}C{=}O)_2$ as the primary organometallic Sn-containing product. The reaction of $\{[(CH_2)Me_2Si]_2N\}_2Sn$ with CS_2 led to formal reduction of CS_2 to $[CS_2]^{2-}$, yielding $[\{[(CH_2)Me_2Si]_2N\}_2Sn]_2CS_2\{[(CH_2)Me_2Si]_2N\}_2Sn$, in which the $[CS_2]^{2-}$ is coordinated through C and S to two tin centers. The product $[\{[(CH_2)Me_2Si]_2N\}_2Sn]_2CS_2\{[(CH_2)Me_2Si]_2N\}_2Sn$ also contains a novel 4-membered Sn−Sn−C−S ring, and exhibits a further bonding interaction through sulfur to a third Sn atom. Reaction of OCS with $\{[(CH_2)Me_2Si]_2N\}_2Sn$ resulted in an insoluble polymeric material. In a comparison reaction, $[(Me_3Si)_2N]_2Sn$ was treated with OCS to yield $Sn_4(\mu_4\text{-}O)(\mu_2\text{-}OSiMe_3)_5(\eta^1\text{-}N{=}C{=}S)$. A combination of NMR and IR spectroscopy, mass spectrometry, and single crystal X-ray diffraction were used to characterize the products of each reaction. The oxygen atoms in the final products come from the facile cleavage of either CO_2 or OCS, depending on the reacting carbon dichalogenide.

Introduction

The use of carbon dioxide, a relatively inert molecule, as a C_1 synthon to produce more valuable organic products has been of growing interest for many years.[1−5] While the vast majority of studies involve transition-metal-mediated transformations, there have been noteworthy studies of main group metal species that react with CO_2 to form organic products. For example, Stephan and co-workers have recently used "frustrated" Lewis acid−base pairs based on aluminum and phosphorus to activate CO_2 for the production of methanol.[6] Several groups have examined, both theoretically and experimentally, the use of tin-based catalysts such as $R_2Sn(OMe)_2$ to form dimethyl carbonate $[(MeO)_2CO]$ from CO_2 and methanol at high pressure and high temperature.[7−10] In addition, one of the most studied CO_2 activation pathways is its insertion into main group- or transition metal−nitrogen bonds to form carbamates.[4] Over the past several years our research group has contributed to this area through investigations of the reactivity of group 2 and 12 metal bis(amides) and bis(silylamides) with CO_2.[11−14] In general, what CO_2-containing products are obtained in these reactions depend primarily on the nature of the substituents attached to the amido ($-NR_2$) ligands. If both R groups are alkyl or aryl moieties, then stable metal carbamates are formed from simple insertion of CO_2

*To whom correspondence should be addressed. E-mail: rakemp@unm.edu.

(1) Aresta, M.; Dibenedetto, A. *Dalton Trans.* **2007**, 2975–2992.
(2) Sakakura, T.; Choi, J.-C.; Yasuda, H. *Chem. Rev.* **2007**, *107*, 2365–2387.
(3) Louie, J. *Curr. Org. Chem.* **2005**, *9*, 605–623.
(4) Belli Dell'Amico, D.; Calderazzo, F.; Labella, L.; Marchetti, F.; Pampaloni, G. *Chem. Rev.* **2003**, *103*, 3857–3897.
(5) Arakawa, H.; Aresta, M.; Armor, J. N.; Barteau, M. A.; Beckman, E. J.; Bell, A. T.; Bercaw, J. E.; Creutz, C.; Dinjus, E.; Dixon, D. A.; Domen, K.; DuBois, D. L.; Eckert, J.; Fujita, E.; Gibson, D. H.; Goddard, W. A.; Goodman, D. W.; Keller, J.; Kubas, G. J.; Kung, H. H.; Lyons, J. E.; Manzer, L. E.; Marks, T. J.; Morokuma, K.; Nicholas, K. M.; Periana, R.; Que, L.; Rostrup-Nielson, J.; Sachtler, W. M. H.; Schmidt, L. D.; Sen, A.; Somorjai, G. A.; Stair, P. C.; Stults, B. R.; Tumas, W. *Chem. Rev.* **2001**, *101*, 953–996.
(6) Ménard, G.; Stephan, D. W. *J. Am. Chem. Soc.* **2010**, *132*, 1796–1797.
(7) Ballivet-Tkatchenko, D.; Chambrey, S.; Keiski, R.; Ligabue, R.; Plasseraud, L.; Richard, P.; Turunen, H. *Catal. Today* **2006**, *115*, 80–87.
(8) Miyake, N.; Nagahara, H.; Bijanto, B.; Wakamatsu, K.; Orita, A.; Otera, J. *Organometallics* **2010**, *29*, 1290–1295.
(9) Kohno, K.; Choi, J.-C.; Ohshima, Y.; Yili, A.; Yasuda, H.; Sakakura, T. *J. Organomet. Chem.* **2008**, *693*, 1389–1392.
(10) Suciu, E. N.; Kuhlmann, B.; Knudsen, G. A.; Michaelson, R. C. *J. Organomet. Chem.* **1998**, *556*, 41–54.
(11) Tang, Y.; Zakharov, L. N.; Rheingold, A. L.; Kemp, R. A. *Organometallics* **2004**, *23*, 4788–4791.
(12) Tang, Y.; Kassel, W. S.; Zakharov, L. N.; Rheingold, A. L.; Kemp, R. A. *Inorg. Chem.* **2005**, *44*, 359–364.
(13) Tang, Y.; Felix, A. M.; Boro, B. J.; Zakharov, L. N.; Rheingold, A. L.; Kemp, R. A. *Polyhedron* **2005**, *24*, 1093–1100.
(14) Tang, Y.; Felix, A. M.; Manner, V. W.; Zakharov, L. N.; Rheingold, A. L.; Moasser, B.; Kemp, R. A. *ACS Symp. Ser.* **2006**, *917*, 410–421.

Published on Web 11/09/2010

Scheme 1. Reaction of $[(Me_3Si)_2N]_2Sn$ (**1**) with CO_2 to Form the Dimer of Bis(trimethylsiloxy)tin, Trimethylsilyl Isocyanate, and 1,3-Bis-(trimethysily)carbodiimide[17]

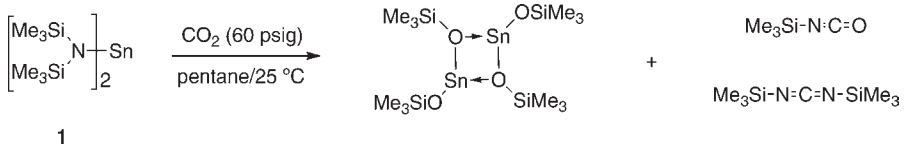

1

Scheme 2. Reaction of **1** with Excess OCS to Produce **3**

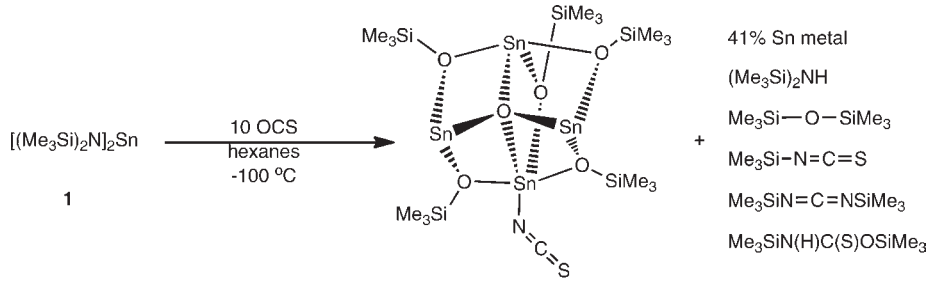

1 3

into the metal−nitrogen bonds, as had been previously noted by Chang and others using a series of magnesium bis-(amides).[15] Using the cyclohexyl (cy) derivative $Mg[N(cy_2)]_2$ with CO_2, we were able to demonstrate the first example of a symmetrically bound η^2-carbamate ligand, a bonding mode that had been postulated not to exist.[11] However, as was seen in the pioneering work of Wannagat et al.,[16] Sita et al.,[17] and Coates et al.,[18,19] when metal complexes of silyl-containing amides such as $-N(R)(SiMe_3)$ or $-N(SiMe_3)_2$ are used in the reaction with CO_2, the initially formed metal carbamates are not thermally stable. They undergo elimination of organic isocyanates and/or carbodiimides to produce metal siloxides as byproducts (Scheme 1).

Surprisingly, treatment of **1** with its heavier analogue CS_2 gave no evidence of reaction, even at elevated temperatures.[20] To probe whether the steric (covalent $radius_{sulfur}$ = 1.05 Å vs covalent $radius_{oxygen}$ = 0.66 Å)[21] or electronic differences between CO_2 and CS_2 were responsible for the extreme variability in reaction chemistry, the series of heterocumulenes CO_2, OCS, and CS_2 was reacted with **1** and bis(2,2,5,5-tetramethyl-2,5-disila-1-azacyclopent-1-yl)tin (**2**), $\{[(CH_2)Me_2Si]_2N\}_2Sn$. Compound **2** is simply a "tied-back" version of **1** and can be easily prepared using the cyclic 2,2,5,5-tetramethyl-2,5-disila-1-azacyclopentane ligand.[22,23] Its use should reduce any repulsive steric interactions that may exist between the bulky $-N(SiMe_3)_2$ ligand and the carbon dichalcogenides, thereby allowing electronic differences to drive the reactivity. To quantify the steric and electronic contributions of **1** and **2** we also utilized density functional theory (DFT) calculations at the B3LYP/LACVP** level.

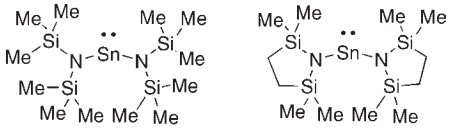

1 2

Results and Discussion

Reaction of 1 with OCS. As noted above, Sita and coworkers have reported the surprising difference in the reactivity of **1** with CO_2 and CS_2.[20] The unexpected lack of reactivity of CS_2 toward **1** was subsequently confirmed by us. This increased our curiousity about the overall reactivities of CX_2 molecules with stannylenes in general, and caused us to examine the reaction of **1** with excess OCS at −100 °C in hexanes (Scheme 2). Upon warming to room temperature the reaction mixture turned from red-orange to pale yellow. After stirring overnight, the reaction was then recooled to −78 °C and excess OCS was removed in vacuo. Metallic tin was separated by filtration, and the crude product was recrystallized from pentane at −22 °C. Colorless crystals of $Sn_4(\mu_4\text{-}O)(\mu_2\text{-}OSiMe_3)_5(\eta^1\text{-}N{=}C{=}S)$ (**3**) were isolated in 39% yield. The supernatant was analyzed by gas chromatography-mass spectrometry (GC-MS) and found to contain several organic byproducts, including $Me_3SiN{=}C{=}S$ and $Me_3SiN{=}C{=}NSiMe_3$. These organic products were expected based on the prior work of Sita et al. describing the reaction of **1** with CO_2.[24]

Initial spectroscopic studies of **3** showed only a single resonance in the ^1H NMR spectrum at 0.23 ppm, and two signals in the ^{13}C NMR spectrum at 3.6 and 176.5 ppm, consistent with the presence of $-Si(CH_3)_3$ groups and $-N{=}C{=}S$. The ^{119} Sn NMR spectrum was

(15) Yang, K.-C.; Chang, C.-C.; Yeh, C.-S.; Lee, G.-H.; Peng, S.-M. *Organometallics* **2001**, *20*, 126–137.
(16) Wannagat, U.; Kuckertz, H.; Krueger, C.; Pump, J. *Z. Anorg. Allg. Chem.* **1964**, *333*, 54–61.
(17) Sita, L. R.; Babcock, J. R.; Xi, R. *J. Am. Chem. Soc.* **1996**, *118*, 10912–10913.
(18) Cheng, M.; Darling, N. A.; Lobkovsky, E. B.; Coates, G. W. *Chem. Commun.* **2000**, 2007–2008.
(19) Cheng, M.; Moore, D. R.; Reczek, J. J.; Chamberlain, B. M.; Lobkovsky, E. B.; Coates, G. W. *J. Am. Chem. Soc.* **2001**, *123*, 8738–8749.
(20) Babcock, J. R. Heterocumulene Metathesis Mediated by Tin(II) Silyl Amides. Ph.D. Dissertation, University of Chicago, Chicago, IL, 1998.
(21) Cordero, B.; Gomez, V.; Plater-Prats, A. E.; Reves, M.; Echererria, J.; Cremades, E.; Barragan, F.; Alvarez, S. *Dalton Trans.* **2008**, 2832–2838.
(22) Westerhausen, M.; Greul, J.; Hausen, H.-D.; Schwarz, W. *Z. Anorg. Allg. Chem.* **1996**, *622*, 1295–1305.
(23) Wrackmeyer, B.; Pedall, A.; Weidinger, J. *Z. Naturforsch., B: Chem. Sci.* **2001**, *56b*, 1009–1014.
(24) Sita, L. R.; Babcock, J. R.; Xi, R. *J. Am. Chem. Soc.* **1996**, *118*, 10912–10913.

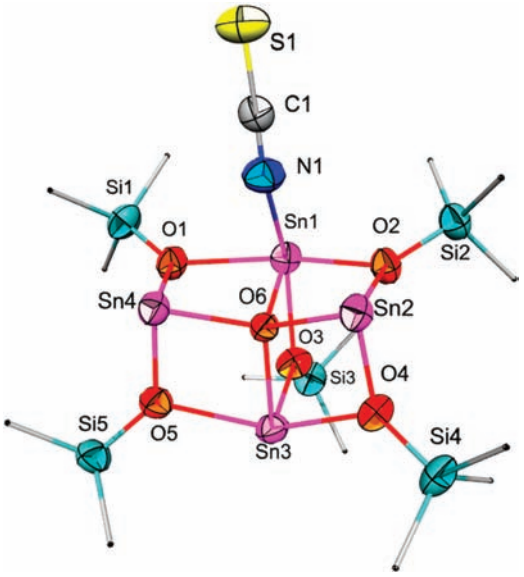

Figure 1. X-ray structure of $Sn_4(\mu_4\text{-}O)(\mu_2\text{-}OSiMe_3)_5(\eta^1\text{-}N{=}C{=}S)$ **3**. For clarity, hydrogen atoms are not shown, and the methyl carbons are shown as sticks.

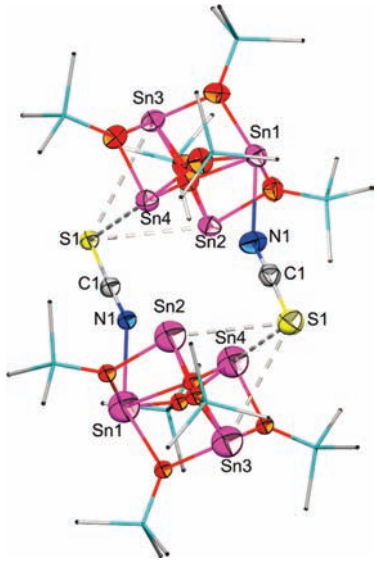

Figure 2. Long-range Sn···S interactions between neighboring molecules of **3**. For clarity, hydrogen atoms are omitted, and trimethylsilyl groups are shown as sticks.

less informative, showing a broad resonance at 107−108 ppm and a sharp singlet at −143 ppm. These signals were significantly upfield from the chemical shift of **1** (766 ppm)[25] and are consistent with a change from Sn−N to Sn−O bonds. After examination of the crystal structure (vide infra), the signals were assigned, respectively, to the three Sn atoms with only O-based ligands and one Sn atom with an −N=C=S ligand. A strong IR absorbance at 2044 cm^{-1} provided further evidence for the −N=C=S functionality.

To be confident of the molecular architecture, a structural determination of **3** was performed by single crystal X-ray diffraction (Figure 1). Despite the isolation of metallic tin as a byproduct, the core of **3** consists of four Sn^{2+} atoms in their original oxidation states. The two tricoordinate Sn atoms, Sn(2) and Sn(4), have virtually identical environments. Each are bound to two O atoms from bridging -$OSiMe_3$ groups, as well as to the central μ_4-O atom, O(6), believed to be generated upon cleavage of OCS (vide infra). The other two Sn atoms, Sn(1) and Sn(3), each bridge three -$OSiMe_3$ ligands in addition to the μ_4-O atom. As well, Sn(1) accommodates the newly generated -N=C=S anion, with a Sn−N bond length of 2.512(5) Å. The presence of -$OSiMe_3$ ligands around the periphery of the Sn_4 cluster is consistent with the previously described insertion/elimination pathways that yield the variety of organic byproducts that are seen in this reaction (Scheme 2).[17]

The central μ_4-O atom in **3** is distorted significantly from idealized tetrahedral geometry. The six Sn−O−Sn bond angles around the central μ_4-O atom are 103.66(17), 103.83(17), 106.88(17), 107.01(18), 107.99(19), and 126.4(2)°. The one unusually large angle of 126.4(2)° is most likely due to the absence of any bridging ligands between Sn(2) and Sn(4). The Sn−O bond lengths of the tricoordinate Sn(2) and Sn(4) atoms to the bridging −$OSiMe_3$ ligands are identical within experimental error, averaging 2.103 Å. The bonds to the μ_4-O atom are only slightly longer at 2.135(3) and 2.141(3) Å for Sn(2) and Sn(4), respectively. More variation is seen at the four-coordinate Sn(3) center. Only one of its three Sn−O bonds is within the range of those described above, that being 2.101(4) Å for Sn(3)−O(3). The other two Sn−O bonds are more than 0.2 Å longer, measuring 2.339(3) and 2.358(4) Å, and are comparable to the Sn−O bond lengths found at Sn(1) that range from 2.309(3) to 2.354(3) Å. The shortest Sn−O bond for Sn(1) is to μ_4-O(6), measuring 2.218 Å. However, this value is significantly longer than any of those formed by Sn(2) and Sn(4).

Inspection of the packing diagram of **3** reveals that the terminal sulfur atom S(1) interacts with the three coordinatively unsaturated tin atoms of a neighboring molecule to form a dimer (Figure 2). Two of these interactions are somewhat shorter, measuring 3.5410(10) Å [Sn(2)−S(1)] and 3.4483(25) Å [Sn(4)−S(1)], while the third is noticeably longer at 3.8473(22) [Sn(3)−S(1)]. All three are well within the sum of the van der Waals radii of Sn (2.16 Å) and S (1.80 Å).[26]

Reaction of 2 with CO_2. Upon exposure to 60 psig of CO_2 at room temperature, a pentane solution of $\{[(CH_2)Me_2Si]_2N\}_2Sn$ **2** underwent immediate reaction, changing in color from red-orange to yellow in less than a minute (Scheme 3). This is significantly more rapid than the comparable reaction of **1** with CO_2,[17] indicating that **2** is much more reactive toward CO_2 than is **1**. This reactivity increase is possibly related to the smaller cone angle of the cyclic $-N[SiMe_2(CH_2)]_2$ligand compared to the open bis(trimethylsilyl)amido ligand (vide infra). No further changes to the reaction solution were observed over approximately 1 h, and the reaction vessel was vented. A sample of the headspace gas was collected for GC-MS analysis, which indicated the presence of CO. The solvent was removed under reduced pressure, and the crude product was extracted into toluene and filtered. The filtrate was cooled to −20 °C for several days and small yellow crystals of **4** were collected. The yield was 50%

(25) Braunschweig, H.; Chorley, R. W.; Hitchcock, P. B.; Lappert, M. F. *J. Chem. Soc., Chem. Commun.* **1992**, 1311–13.

(26) Bondi, A. *J. Phys. Chem.* **1964**, *68*, 441–451.

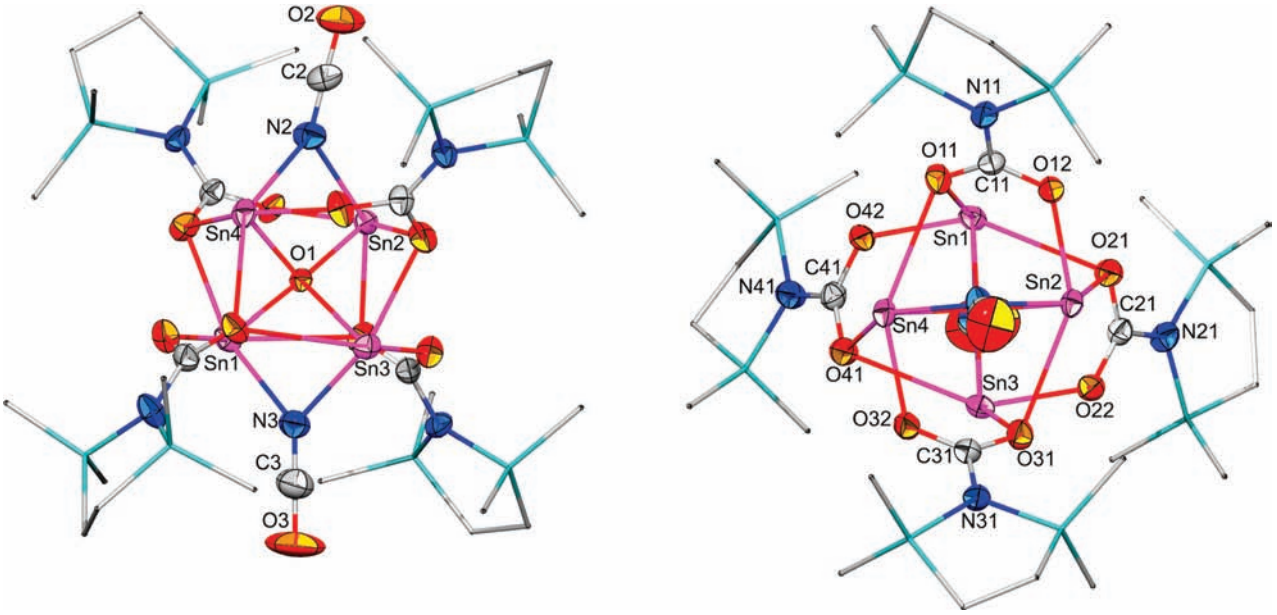

Figure 3. Two views of the molecular structure of $Sn_4(\mu_4\text{-}O)\{\mu_2\text{-}O_2CN[SiMe_2(CH_2)_2]\}_4(\mu_2\text{-}N{=}C{=}O)_2$ **4**. Thermal ellipsoids are shown at 50% probability. For clarity, silicon and carbon atoms (except C2 and C3) are shown as sticks, and hydrogen atoms have been omitted. In the view on the right the observer looks down the approximately linear isocyanate axes.

Scheme 3. Reaction of **2** with CO_2 to Produce **4**

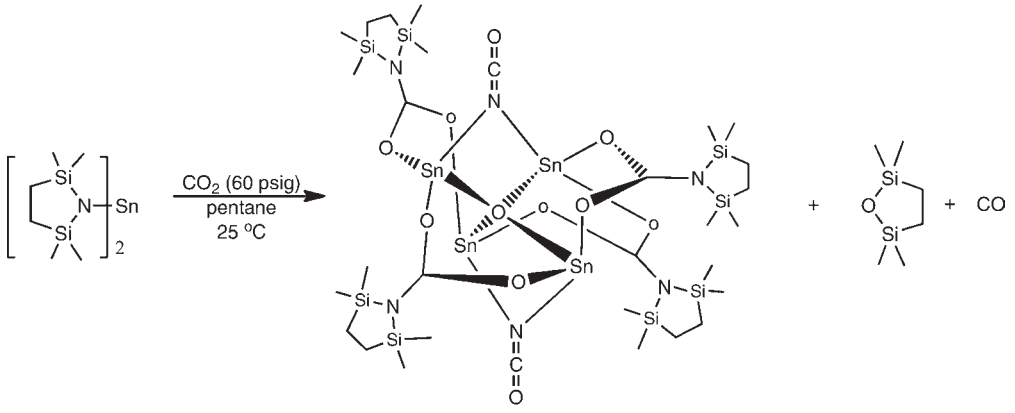

2 4

based on tin. Analysis of the mother liquor by GC-MS showed that the major organic byproduct of the reaction was the cyclic ether 2,2,5,5-tetramethyl-2,5-disila-1-oxacyclopentane, $[(CH_2)Me_2Si]_2O$.

The ^1H NMR spectrum of **4** exhibited singlets at 0.24 and 0.71 ppm, indicating the presence of the methyl and methylene groups of the $-N[SiMe_2(CH_2)]_2$ ligand. The $^{13}C\{^1H\}$ NMR spectrum was more informative, showing resonances for the methyl and methylene groups at −0.41 and 8.39 ppm, respectively, along with two other downfield signals at 167.4 and 180.5 ppm. These resonances were found to correspond to the carbons of the $-O_2C$ carbamate and $-N{=}C{=}O$ isocyanate groups, respectively. The IR spectrum of **4** showed strong absorbances for the isocyanate at 2171 and 2277 cm^{-1}. At room temperature only one resonance at −316 ppm was observed in the ^{119}Sn NMR, indicating the presence of only one type of Sn center. The identity of **4** was determined by single crystal X-ray diffraction (Figure 3) as $Sn_4(\mu_4\text{-}O)\{\mu_2\text{-}O_2CN[SiMe_2(CH_2)]_2\}_4(\mu_2\text{-}N{=}C{=}O)_2$.

Compound **4** consists of a highly symmetrical cluster with a $[\mu_4\text{-}O]Sn_4$ core, similar to that found in **3**. Two bridging isocyanates are present as suggested by the spectroscopic data. One of the striking features of **4** is its pseudo 4-fold symmetry down the O=C=N−O−N=C=O axis (Figure 3, right). The two O=C=N bond angles are linear [179.2(6) and 179.4(7)°] as is the N(2)-[μ_4-O(1)]−N(3) angle (179.1°). The μ_4-O(1) is essentially tetrahedral with Sn−O−Sn angles between 107.48(9) and 112.64(10)°. These Sn−O−Sn angles fall within a much narrower range than other structurally characterized $[\mu_4\text{-}O]M_4$ clusters,[27] including **3**. In contrast to compound **3**, the bonds between the μ_4-O and the Sn atoms in **4** are all 2.180 Å, identical within experimental error.

The coordination spheres of the Sn atoms, all of which remain Sn^{2+}, are completed by four new silyl-substituted carbamato ligands formed by insertion of CO_2 into the Sn−N bonds of **2**. Each carbamate ligand is bound to

(27) Cambridge Structural Database, version 5.31. See: Allen, F. H. *Acta Crystallogr.* **2002**, *B58*, 380–388.

Scheme 4. Reaction of **2** with CS_2 to Produce **5**

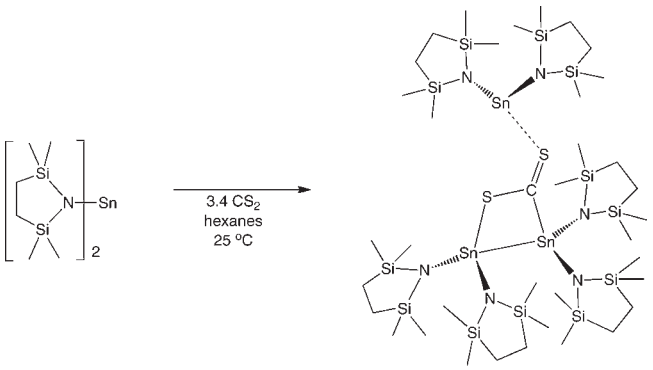

2 **5**

three Sn atoms via two relatively short Sn−O bonds and one longer Sn−O interaction in a μ_3,η^3 pattern. As would be expected, the primary Sn−O bonds of the bridging μ_2-O of each carbamate [Sn(1)−O(11), Sn(2)−O(21), Sn(3)−O(31), and Sn(4)−O(41)] are longer [2.331(3) to 2.458(3) Å] than those made by the singly coordinated oxygen atoms [2.164(3) to 2.226(3) Å]. The secondary Sn−O interactions for the μ_2-O atoms range from 2.716(3) to 2.835(3) Å.

The only previous example of this carbamate ligand was reported nearly 30 years ago by Andersen in a hafnium-containing complex.[28] The Hf complex was characterized only by IR and NMR spectroscopy, thus making **3** the first structurally characterized example of a silyl-substituted carbamate. To the best of our knowledge, no other silyl-substituted carbamates have been reported.[29] This is somewhat surprising given the ubiquitous nature of alkyl and/or aryl-substituted carbamates and the widespread use of silylamines such as $-N(SiMe_3)_2$ as ligands for both main group and transition metal compounds. However, the scarcity of these species supports the observations that have been made regarding the preference for transient formation of silyl-substituted carbamates with subsequent elimination of isocyanates or other organic products.[14,16−18]

As was mentioned above, analysis of the reaction headspace gas via GC-MS indicated the presence of CO. In a separate experiment, CO_2 from the lecture bottle was analyzed by GC-MS to determine whether a low level of CO was present; none was found. Since this reaction was done under rigorously anhydrous conditions, this strongly implies that one of the oxygen atoms from the CO_2 is utilized to form the $[(CH_2)Me_2Si]_2O$ co-product that is also observed by GC-MS. As well, this suggests that the source of the μ_4-O atom at the center of this Sn cluster also derives from facile cleavage of CO_2, and not from adventitious O_2 or H_2O.[30] Likewise, it suggests that the μ_4-O atom in **3** was similarly obtained from the OCS reagent, although we never detect side products derived from the expected and highly reactive [CS] fragment. The observation that the yields of both **3** and **4** are both high and reproducible provides further support for this argument.

Reaction of 2 with OCS. When a petroleum ether solution of **2** was exposed to 2 equiv of OCS under reaction conditions similar to those used to form **3**, the ensuing reaction was rapid and produced an insoluble red-brown material. This material was collected by filtration, but efforts to determine its solid-state structure were unsuccessful because of the insolubility of the product(s) in solvents including D_2O, petroleum ether, pentane, diethyl ether, tetrahydrofuran (THF), methylene chloride, acetonitrile, toluene, and pyridine. The lack of solubility of this compound also precluded characterization by solution NMR techniques. Absorbances in the IR spectrum at 2277 and 2066 cm^{-1} suggested the presence of −N=C=O and −N=C=S functional groups. Elemental analysis revealed that the material contains 52% Sn, as well as smaller amounts of carbon, hydrogen, nitrogen, and sulfur. Under no reaction conditions were we able to produce crystalline material either directly or via recrystallization. The only product detected in the supernatant solution by GC-MS was $((CH_2)Me_2Si)_2O$, as had been seen in reaction of **2** with CO_2 to form **4**.

Reaction of 2 with CS_2. The final reaction in this series is that of **2** with CS_2 (Scheme 4). Recall that **1** reacts with CO_2 and OCS but shows no reactivity toward CS_2.[20] However, addition of excess CS_2 to a hexanes solution of **2** produced an immediate reaction. The color progressed from the deep red-orange of **2**, through a pale red-orange, and eventually to dark green after completion of the CS_2 addition. The reaction was allowed to stir for 1 h at room temperature, after which the volatiles were removed under vacuum and crystals began to form. The crude reaction mixture was cooled to −20 °C overnight. Dark green crystals of **5** were isolated in essentially quantitative yield after drying under vacuum.

The ^1H NMR spectrum of **5** showed resonances at 0.05 and 0.83 ppm for the methyl and methylene protons, respectively. The $^{13}C\{^1H\}$ NMR exhibited resonances for the methyl and methylene carbons at 3.09 and 10.58 ppm. The *C*S_2 carbon resonance was not observed, despite the fact that the IR spectrum suggested the presence of a C=S functional group with absorbances at 1523 and 869 cm^{-1}. The ^{119}Sn NMR exhibited three resonances at 18.0 (sharp singlet), 83.5 (sharp singlet), and 363 (broad) ppm. Since the exact structural composition of **5** could not be unambiguously determined from the spectroscopic data, a single crystal X-ray diffraction analysis was performed.

The structure of **5** is shown in Figure 4, and consists of two molecules of **2** joined by a bridging CS_2 through the C(1) and S(1) of the CS_2. This cluster forms a planar, four-membered ring of Sn(1)−Sn(2)−C(1)−S(1), and this plane when extended also contains S(2). The C(1)−S(1) and C(1)=S(2) bond lengths of 1.717(3) and 1.640(3) Å reflect the fact that this fragment has undergone reduction, as does the decrease in the S(1)−C(1)−S(2) angle to 124.10(17)°. The Sn atoms Sn(1) and Sn(2), which form a Sn−Sn bond measuring 2.8289(4) Å, appear to have been *formally* oxidized to Sn^{3+}, along with a concomitant reduction of CS_2 to a $[S=C-S]^{2-}$ species. A similar formal oxidation to Sn^{3+} was reported by Gade and colleagues[31] for a hexaaminodistannane molecule.

(28) Andersen, R. A. *Inorg. Chem.* **1979**, *18*, 2928–2932.

(29) Two silyl-substituted carbamate esters have been reported. Their formation did not involve carbon dioxide. See: Morton, D. W.; Neilson, R. H. *Organometallics* **1982**, *1*, 623–627. Pitt, C. G.; Skillern, K. R. *Inorg. Chem.* **1967**, *6*, 865–870.

(30) McCowan, C. S.; Groy, T. L.; Caudle, M. T. *Inorg. Chem.* **2002**, *41*, 1120–1127.

(31) Lutz, M.; Haukka, M.; Pakkanen, T. A.; Gade, L. H. *Z. Anorg. Allg. Chem.* **2003**, *629*, 182–184.

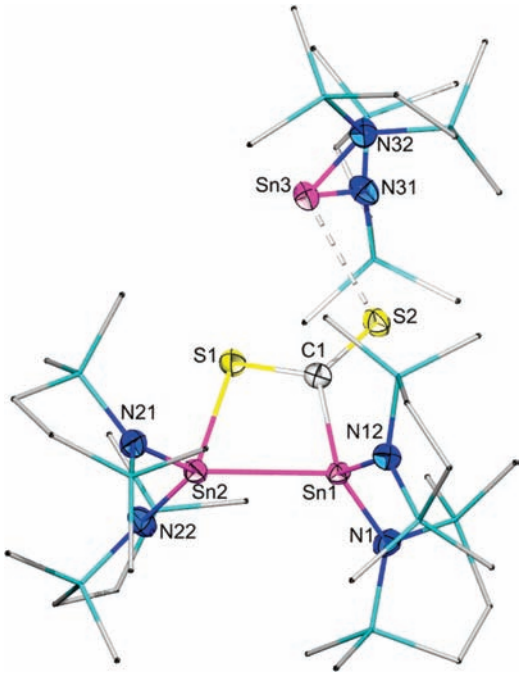

Figure 4. Molecular structure of $[[((CH_2)Me_2Si)_2N]_2Sn]_3 \cdot CS_2$ **5**. For clarity, the silicon and carbon atoms (other than C1) are shown as sticks, and hydrogen atoms have been omitted.

The Sn−Sn bond length of Gade's distannane measured 2.8204(4) Å, in very good agreement with **5**. The Sn−N bond lengths for Sn(1)−N(1) and Sn(2)−N(12) are noticeably shorter [2.021(2)−2.025(3) Å] than those of Sn(3)−N(31) and Sn(3)−N(32) at 2.089(3) Å, consistent with the higher formal oxidation state of Sn(1) and Sn(2).[31] The N−Sn−N bond angles around Sn(1) and Sn(2) are larger, measuring 111.44(10) and 109.89(11)°, respectively, while the N−Sn−N bond angle for Sn(3) is 99.81(10)°. The overall geometries around Sn(1) and Sn(2) are best described as distorted tetrahedral arrangements with no stereochemically active lone pairs. This is consistent with their formal Sn^{3+} oxidation state.

The remaining Sn^{2+} atom Sn(3) forms a dative bond with the pendant S(2) atom, with an S(2)−Sn(3) distance of 3.0067(9) Å. This distance is significantly longer than the covalent Sn(2)−S(1) bond length (2.5174(7) Å), but much shorter than the intermolecular Sn···S distances in **3** (3.45−3.85 Å). This dative interaction in **5** can be regarded as donation of a lone pair of electrons from S into the empty p-orbital of stannylene **2**, which is isolobal with a carbene.[32] The extra electron density at Sn(3) can be seen in the upfield shift of ~445 ppm in the ^{119}Sn NMR, from 808 ppm for the free stannylene **2** to 363 ppm in **5**.

It is particularly noteworthy that further treatment of **5** with CS_2 does not change the coordination environment. No more CS_2 can be added to the complex even upon heating to 40 °C in the presence of a 10-fold excess of CS_2. Interestingly, the third stannylene, which is held in place only by the long S(2)−Sn(3) dative bond, is surprisingly robust and does not cleave and undergo further reaction with excess CS_2. Because the $[CS_2]^{2-}$ is covalently bound to the two oxidized Sn atoms, it is not surprising that this fragment cannot be removed under vacuum or by heating in a closed vessel.

DFT Calculations. In an effort to better understand the differences in reactivity of the tin(II) silylamides **1** and **2** with this series of carbon dichalcogenides, DFT calculations were performed on both tin complexes. The Jaguar 7.0 program[33] was used to fully optimize all the structures at the B3LYP[34,35] level of theory, using the LACVP** basis set (the Hay and Wadt effective core potential basis set[36] LANL2DZ** for the tin atom and the 6-31G** basis set[37,38] for all other atoms). The optimized geometries were compared to each other as well as to experimental values to quantify the steric contributions of the ligands around the Sn centers.[39,40] This included the calculation of cone angles for both $-N(SiMe_3)_2$ and the "tied back" $-N[SiMe_2(CH_2)]_2$ ligands. Finally, we were also able to compare calculated electron densities on the Sn and N atoms of both **1** and **2** to eliminate the possibility that the observed differences in reactivity were due to electronic differences.

The bond lengths and angles arising from the DFT calculations for **1** generally compare favorably to the experimental measurements (Table 2);[39,40] however, there are some notable differences. Most significantly, the calculated N−Sn−N bond angle (107.2°) for **1** is larger than the angles found experimentally, both in the solid-state (104.7°) and gas phase (96°). A priori, one would expect the DFT calculations to be more similar to the gas-phase electron diffraction structure than to the solid-state X-ray structure, which possibly is constrained by crystal packing forces. The discrepancies in the calculated and measured N−Sn−N bond angles are even more pronounced for **2**, although the measured bond angle comes from the loosely bound molecule of **2** found in **4** and not from a molecule of pure **2**, which has not been structurally characterized. The calculated N−Si bond lengths were also slightly longer than the measured lengths for both Sn complexes, with the larger deviation again being observed in the cyclic species **2**.

We chose to study the $-N[SiMe_2(CH_2)]_2$ ligand because previous studies of this ligand in transition metal[41] and lanthanide[42] complexes have been described by Rees and Just to be less sterically hindered than the bis(trimethylsilyl)amido ligand. This conclusion is supported by our initial calculations. As shown in Figure 5, there is a large difference of about 22° in the cone angles between the $-N(SiMe_3)_2$ and $-N[SiMe_2(CH_2)]_2$ ligands (144.5° and 122.9°, respectively). This is due to the "tied back" nature of the $-N[SiMe_2(CH_2)]_2$ ring, and is also clearly seen in the difference of more than 10° between the

(32) Mansell, S. M.; Russell, C. A.; Wass, D. F. *Inorg. Chem.* **2008**, *47*, 11367–11375.

(33) *Jaguar*, 7.0; Schrödinger LLC: New York, 2007.
(34) Becke, A. D. *J. Chem. Phys.* **1993**, *98*, 5648–5652.
(35) Lee, C.; Yang, W.; Parr, R. G. *Phys. Rev. B: Condens. Matter* **1988**, *37*, 785–789.
(36) Hay, P. J.; Wadt, W. R. *J. Chem. Phys.* **1985**, *82*, 299–310.
(37) Franci, M. M.; Pietro, W. J.; Hehre, W. J.; Binkley, J. S.; Gordon, M. S.; DeFrees, D. J.; Pople, J. A. *J. Chem. Phys.* **1982**, *77*, 3654–3665.
(38) Hehre, W. J.; Ditchfield, R.; Pople, J. A. *J. Chem. Phys.* **1972**, *56*, 2257–2261.
(39) Fjeldberg, T.; Hope, H.; Lappert, M. F.; Power, P. P.; Thorne, A. J. *J. Chem. Soc., Chem. Commun.* **1983**, 639–41.
(40) Lappert, M. F.; Power, P. P.; Slade, M. J.; Hedberg, L.; Hedberg, K.; Schomaker, V. *J. Chem. Soc., Chem. Commun.* **1979**, 369–70.
(41) Just, O.; Gaul, D. A.; Rees, W. S., Jr. *Polyhedron* **2001**, *20*, 815–821.
(42) Just, O.; Rees, W. S., Jr. *Inorg. Chem.* **2001**, *40*, 1751–1755.

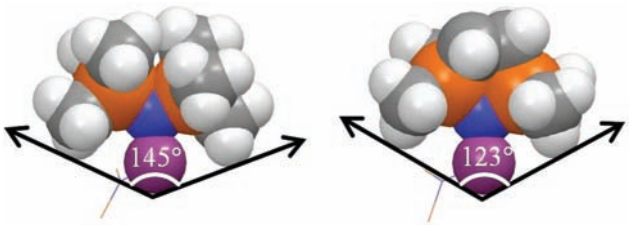

Figure 5. Relative steric demands of the ligands in bis[bis(trimethylsilyl)amido]tin (left) and bis(2,2,5,5-tetramethyl-2,5-disila-1-azacyclopent-1-yl)tin (right) complexes. The tin atom and one ligand on each molecule are shown in a space-filling model; for clarity, only the nitrogen and silyl atoms of the second ligand are shown.

Si−N−Si angles of the two ligands. The smaller cone angle of the $-N[SiMe_2(CH_2)]_2$ ligand relative to the $-N(SiMe_3)_2$ ligand allows better access to the reactive Sn and N centers and may explain the differences in reactivity between **1** and **2** with these heterocumulenes. Despite the obvious steric differences, the electronic similarities of the ligands are evident upon examination of the calculated partial charges on the Sn, N, and Si atoms, which are virtually identical for the two systems, thus indicating that our initial hypothesis that these two complexes would be electronically similar is correct.

To more fully understand the bonding in the distannane **5**, DFT calculations were performed. The relative charges of the three tin metal centers suggest that two of the tin molecules in **5** have added across the C=S bond while the third tin molecule is only very loosely bound to the distannane-CS_2 complex. The tin atom on the loosely coordinated molecule has a calculated partial charge of +0.86 e. When compared to the calculated partial charge of +0.85 e for the free molecule, this confirms that the loosely coordinated tin molecule contributes very little electron density to the distannane-CS_2 complex. The two remaining tin centers in **5** are significantly more electropositive than the tin atom in the free tin amide: Sn(2), the tin atom connected to sulfur, has a calculated partial charge of +0.98 e and Sn(1), the tin atom connected to carbon, has a calculated partial charge of +1.24 e. C(1) and S(1) are correspondingly more electronegative than in CS_2.

DFT calculations were also performed on the series of carbon dichalcogenides CO_2, OCS, and CS_2, at the B3LYP/LACVP** level to quantify the differences in central-carbon-atom electron densities and bond lengths across the series. As expected, CO_2 has the most electropositive central carbon atom (+0.64 e vs +0.29 e for OCS and −0.04 e for CS_2), and the shortest C=E bond lengths in the series. These results are consistent with the results of Yates and co-workers[43] for the partial charges of CS_2 and Matsubara and Hirao[44] for CO_2. If the reaction of the tin(II) silylamide with the carbon dichalcogenide is initiated by attack of the electronegative nitrogen atom on the electropositive carbon atoms of CO_2, CS_2, or OCS, then one would expect CO_2 to be the most reactive of the carbon dichalcogenides. The fact that CO_2 reacts completely with both **1** and **2** as does OCS, whereas CS_2 fails to react with **1** and forms a complex with **2**, is consistent with these computational results.

(43) Ariafard, A.; Brookes, N. J.; Stranger, R.; Yates, B. F. *J. Am. Chem. Soc.* **2008**, *130*, 11928–11938.
(44) Matsubara, T.; Hirao, K. *Organometallics* **2001**, *20*, 5759–5768.

Conclusions

We have shown that although the silylamides **1** and **2** are essentially electronically identical, their reactivities with the carbon dichalcogenides CO_2, OCS, and CS_2 are markedly different, suggesting that steric interactions play important roles in these reactions. Use of the slightly smaller $-N(SiMe_2(CH_2))_2$ ligand in place of the well-known $-N(SiMe_3)_2$ ligand provides an overall more reactive tin species. The reaction of **2** with CO_2 was rapid, converting two $-N(SiMe_3)_2$ groups into isocyanate groups, and yielded a $(\mu_4\text{-O})Sn_4$ cluster $-Sn_4(\mu_4\text{-O})(\mu_2\text{-O}_2C[N(SiMe_2(CH_2))_2])_4(\mu_2\text{-N=C=O})_2$ **4**. Two of the tin atoms in the cluster are bound to two −N=C=O ligands through the nitrogen atoms, and the complex also contains the first structurally characterized example of a silyl-substituted carbamate. Most interestingly, the CO observed in the headspace of the reaction strongly suggests that facile cleavage of CO_2 had occurred to produce **4**.

The reaction of **2** with OCS was rapid and gave an insoluble, likely polymeric, material that could not be conclusively characterized. The rapidity of the reaction was not entirely unexpected. The reduction in steric congestion at the Sn−N centers likely allowed for easier attack at these reactive centers by the OCS.

The reaction of **2** with CS_2 yielded the highly unusual, dark green complex **5**, consisting of a cluster of three $\{[(CH_2)Me_2Si]_2N\}_2Sn$ molecules coordinated to one CS_2 molecule that has been formally reduced to $(CS_2)^{2-}$. The decreased steric congestion around the Sn centers has allowed for the complexation of the CS_2 moiety to Sn atoms, but because of the decreased electrophilicity of the carbon in the CS_2 no Sn−N bonds have been broken.

Finally, the reaction of **1** with OCS led to the formation of $Sn_4(\mu_4\text{-O})(\mu_2\text{-OSiMe}_3)_5(\eta^1\text{-N=C=S})$ **3**. As in the formation of **4**, the central bridging oxygen atom appears to come from cleavage of the heterocumulene. The presence of $-OSiMe_3$ ligands around the periphery of the Sn_4 cluster of **3** instead of the carbamate ligands seen in **4** is consistent with the insertion/elimination pathways that yield the variety of organic byproducts also seen in this reaction.

Experimental Section

All manipulations were carried out in an argon-filled glovebox or by using standard Schlenk techniques. Anhydrous solvents were purchased from Aldrich or the Fischer Scientific Company, after which they were stored in the glovebox. Bis[*N,N*′,-bis(trimethylsilyl)amido]tin(II) (**1**) was purchased from the Aldrich Chemical Co. and 2,2,5,5-tetramethyl-2,5-disila-1-azacyclopentane was purchased from Gelest, Inc.; both were used without further purification. ^1H, $^{13}C\{^1H\}$, and $^{119}Sn\{^1H\}$ NMR spectra were obtained on a Bruker AMX 250 spectrometer and were referenced to residual solvent downfield of TMS (^1H and $^{13}C\{^1H\}$), or to external $SnMe_4$ ($^{119}Sn\{^1H\}$). GC-MS data were obtained on a Hewlett-Packard Model 5890/5972A Series. IR spectra were recorded on a Bruker Vector 22 MIR spectrometer. Elemental analyses were performed at Columbia Analytical Services, Inc., 3860 S. Palo Verde Road, Tucson, AZ 85714.

Bis(2,2,5,5-tetramethyl-2,5-disila-1-azacyclopent-1-yl)tin (2). Procedures similar to those reported by Wrackmeyer et al.[23] and Westerhausen et al.[22] were followed. Under argon, 2,2,5,5-tetramethyl-2,5-disila-1-azacyclopentane (6.00 g, 37.60 mmol) was dissolved in 50 mL of diethyl ether then cooled to 0 °C. *n*-Butyllithium (2.5 *M* in hexanes, 15.0 mL, 37.6 mmol) was added dropwise, and the mixture was allowed to warm to room

Table 1. Crystallographic Data and Parameters for Compounds **3**, **4**, and **5**

	3	4	5
empirical formula	$C_{16}H_{45}NO_6SSi_5Sn$	$C_{30}H_{64}N_6O_{11}Si_8Sn_4$	$C_{37}H_{96}N_6S_2Si_{12}Sn_3$
Fw	994.80	1384.35	1382.47
T, K	223(2)	273(2)	228(2)
cryst size (mm)	0.27 × 0.27 × 0.07	0.575 × 0.345 × 0.23	0.41 × 0.39 × 0.23
cryst syst	monoclinic	monoclinic	triclinic
space group	$P2(1)/c$	$P2(1)/n$	$P\bar{1}$
a, Å	15.7984(10)	21.7653(13)	11.6460(11)
b, Å	12.5326(8)	12.5964(9)	17.4939(16)
c, Å	19.7492(13)	22.5189(13)	18.1905(17)
α, deg			112.364(4)
β, deg	130.152(4)	115.917(2)	98.788(4)
γ, deg			97.166(4)
volume, Å^3	3807.7(4)	5553.0(6)	3318.5(5)
Z	4	4	2
calc. density, g/cm^3	1.735	1.656	1.384
μ (MoK$_\alpha$), mm^{-1}	2.831	2.001	1.429
R1[$I > 2\sigma(I)$][a]	0.0345	0.0322	0.0243
wR2[$I > 2\sigma(I)$][b]	0.0821	0.0820	0.0725

[a] $R1 = \sum||F_o| - |F_c||/\sum|F_o|$. [b] $wR2 = \{\sum w(F_o^2 - F_c^2)^2/\sum w(F_o^2)^2\}^{1/2}$.

temperature over a 2 h period with stirring. The resulting solution was added dropwise through a cannula to a solution of tin dichloride (3.58 g, 19.0 mmol) in 50 mL of a mixture of THF/Et_2O held at 0 °C. The reaction mixture was allowed to warm to room temperature while stirring overnight. The lithium chloride precipitate was filtered using a glass frit and Celite as a filtering aid. The solvent was removed from the filtrate at reduced pressure, and the crude product was distilled at reduced pressure (45 μHg). The product was collected between 87−100 °C as a red oil. Yield: 5.18 g (63%). ^{1}H NMR (250 MHz, C_6D_6) δ 0.76 (s, 4H, CH_2), 0.18 (s, 6H, CH_3) ppm. ^{13}C{^{1}H} NMR (63 MHz, C_6D_6) δ 11.57 (s, *C*H$_2$), 4.04 (s, *C*H$_3$) ppm. ^{119}Sn{^{1}H} (93 MHz, C_6D_6) δ 808 (Lit. δ = 798[23] or 821[22]) ppm.

Reaction of Bis[bis(trimethylsilylamido)]tin(II) (1) with OCS to Give Sn$_4$(μ_4-O)(μ_2-OSiMe$_3$)$_5$(η^1-N=C=S) (3). Under argon, a Fisher Porter tube (fitted with a 120 psig pressure relief valve for safety) was loaded with $[(Me_3Si)_2N]_2Sn$ (1.44 g; 3.28 mmol) and dissolved in hexanes (2 g). To this system was attached a 74 cc stainless steel bomb. The solution was cooled to −100 °C and evacuated to remove the argon. The bomb was charged with 60 psig of OCS which was then condensed into the cooled $[(Me_3Si)_2N]_2Sn$/hexanes solution. This was repeated once more with 60 psig and then 20 psig to give a total of 140 psig of OCS (30.3 mmol). The reaction mixture was allowed to stir and slowly warm to 25 °C where it changed color from orange to yellow. The reaction was allowed to stir overnight at room temperature to eventually give a dark brown, cloudy solution. This solution was cooled to −78 °C, and the excess OCS was removed under vacuum (alternatively the OCS can be removed under a stream of argon). The crude product obtained consisted of a black oil and solids (in some reactions a tin mirror was deposited on the sides of the glass vessel). The crude product was filtered and washed with pentane to give a black powder (0.15 g, Sn metal). From the pentane washings, colorless crystals of Sn$_4$(μ_4-O)(μ_2-OSiMe$_3$)$_5$(η^1-N=C=S) were obtained (0.31 g; 39% based on Sn; mp 192−193 °C dec.; slight color change to tan at 160 °C). The volatiles were removed from the filtrate under an argon purge and analyzed by GC-MS. The byproducts were found to be the following: $Me_3SiOSiMe_3$; $(Me_3Si)_2NH$; $Me_3SiN{=}C{=}S$; $Me_3SiN(H)C(S)OSiMe_3$; $Me_3SiN{=}C{=}N\text{-}SiMe_3$. The byproducts were not quantified. ^{1}H NMR (250 MHz, $CDCl_3$) δ 0.23 (s, CH_3) ppm. ^{13}C{^{1}H} NMR (63 MHz, $CDCl_3$) δ 176.52 (N-*C*-S), 3.63 (*C*H$_3$) ppm. ^{119}Sn{^{1}H} (93 MHz, $CDCl_3$, ref to Me_4Sn) δ 108−107 (broad mult), −143 (s) ppm. IR (Nujol): ν = 2044 (s), 1263 (s), 1249 (s), 871 (s), 838 (s), 751 (s) cm^{-1}. Anal. Calcd for $C_{16}H_{45}NO_6SSi_5Sn_4$ (M_W = 994.86): C, 19.32; H, 4.56; N, 1.41. Found: C, 19.03; H, 4.04; N, 1.35.

Reaction of Bis(2,2,5,5-tetramethyl-2,5-disila-1-azacyclopent-1-yl)tin (2) with CO$_2$ to Give Sn$_4$(μ_4-O){μ_2-O$_2$CN[SiMe$_2$(CH$_2$)]$_2$]$_4$}(μ_2-N=C=O)$_2$ (4). In an argon-purged Fisher Porter reactor tube, bis(2,2,5,5-tetramethyl-2,5-disila-1-azacyclopent-1-yl)tin (0.20 g, 0.45 mmol) was dissolved in 20 mL of anhydrous pentane at room temperature. The bottle was charged with CO_2 (60 psig) and allowed to react for approximately an hour. The solvent was removed at reduced pressure, and the crude product was extracted with toluene, filtered, and cooled to −20 °C. After several days at low temperature yellow crystals were obtained. The crystals were isolated and identified as Sn$_4$(μ_4-O){μ_2-O$_2$CN[SiMe$_2$(CH$_2$)]$_2$]$_4$}(μ_2-N=C=O)$_2$ **4** (0.08 g, yield 50% based on tin, mp 102−104 °C). ^{1}H NMR (250 MHz, C_6D_6) δ 0.71 (s, 16H, CH_2), 0.40 (s, 24H, Si(CH_3)$_2$) ppm. ^{13}C{^{1}H} NMR (63 MHz, C_6D_6) δ 180.5 (N=*C*=O), 167.9 (*C*O$_2$), 8.4 (CH_2), −0.4 (CH_3) ppm. ^{119}Sn{^{1}H} (93 MHz, C_6D_6) δ −316 ppm. IR (Nujol): ν = 2277 (w), 2171 (s). Anal. Calcd for $C_{30}H_{64}N_6O_{11}Si_8Sn_4$ (M_w = 1384.39): C, 26.03; H, 4.66 N; 6.07. Found: C, 25.82; H, 4.62; N, 3.98. The predominant byproduct from the mother liquors was 2,2,5,5-tetramethyl-2,5-disila-1-oxacyclopentane and was identified by GC-MS. (Calcd for $C_6H_{16}OSi_2$, 160.4). GC-MS m/z (relative intensity, ion): 160 (16%, M$^+$), 145 (100%, M$^+$ − CH$_3$), 117 (100%, $Me_3SiO(CH_2)_2^+$), 73 (90%, $CH_3SiOCH_2^+$).

Reaction of Bis(2,2,5,5-tetramethyl-2,5-disila-1-aza-cyclopent-1-yl)tin (2) with OCS. Under an argon atmosphere, a solution of bis(2,2,5,5-tetramethyl-2,5-disila-1-aza-cyclopent-1-yl)tin (0.54 g, 1.20 mmol) and petroleum ether (3 g) was cooled to −78 °C and then evacuated to remove the argon. At −78 °C carbonyl sulfide (2.4 mmol) was condensed into the reaction vessel. As the reaction warmed to room temperature a red-brown precipitate formed. The precipitate was filtered from solution and washed several times with petroleum ether. Upon drying 0.15 g of a rust-colored solid was collected. IR (Nujol): ν = 2277 (m), 2066 (s), 1972 (m), 1255 (m) 1054 (m), 794 (m) cm^{-1}. Elemental analysis of C, H, N, S, and Sn gave: C, 11.92; H, 1.74; N, 6.48; S, 17.7; Sn, 52.4. The GC-MS of the filtrate indicated petroleum ether and 2,2,5,5-tetramethyl-2,5-disila-1-oxacyclopentane (Calcd for $C_6H_{16}OSi_2$, 160.4). (GC-MS m/z (relative intensity, ion) 160 (10%, M$^+$), 145 (100%, M$^+$ − CH$_3$).

Reaction of Bis(2,2,5,5-tetramethyl-2,5-disila-1-aza-cyclopent-1-yl)tin (2) with CS$_2$ to Give (5). To a solution of bis-(2,2,5,5-tetramethyl-2,5-disila-1-azacyclopent-1-yl)tin (1.50 g, 3.44 mmol) in hexane (7 g) held at room temperature, CS_2 (1.0 mL, 13.1 mmol) was added dropwise. The reaction was immediate with the color changing from red-orange to dark green. The reaction was allowed to stir for 1 h. Volatiles were removed until crystallization began to occur. The dark green

Table 2. DFT Calculation Results (B3LYP/LACVP**) for Tin Silylamides and Comparisons to the Solid-State X-ray and Gas Phase Electron Diffraction Results

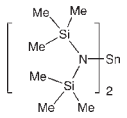

bis[*N*,*N*′-bis(trimethylsilyl)amino]tin(II) $[(Me_3Si)_2N]_2Sn$ (**1**)

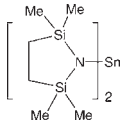

bis(2,2,5,5-tetramethyl-1-aza-2,5-disilacyclopent-1-yl)tin(II) $\{[(CH_2)Me_2Si]_2N\}_2Sn$ (**2**)

	DFT	X-ray[39]	elect. diff.[40]	DFT	X-ray*
Sn−N bond length (Å)	2.09	2.0952(11), 2.0868(18)	2.09	2.07	2.092(3), 2.093(3)
N−Si bond lengths (Å)	1.77	1.7434(16), 1.7453(26). 1.7456(9), 1.7544(14)	1.74	1.78	1.727(4), 1.729(4), 1.733(3), 1.738(4)
N−Sn−N angle (deg)	107.2	104.714(29)	96	107.1	99.91(13)
Si−N−Si angles (deg)	120.2, 120.6	120.927(44), 121.944(28)		109.4, 109.4	108.82(19), 109.09(19)
Si−N−Sn-N dihedral angles (deg)	34.6, 37.3, 48.2, 52.4	35.872(37), 36.145(37), 47.809(53), 50.653(52)		21.4, 22.3, 43.2, 44.0	22.169(205), 35.406(220), 42.602(273), 69.515(229)
ligand cone angle (deg)	144.4, 144.6			122.8, 123.1	
charge on Sn (e)	0.87			0.85	
charge on N (e)	−1.05, −1.05			−1.04, −1.04	
charge on Si (e)	0.89, 0.89, 0.90, 0.90			0.84, 0.84, 0.88, 0.89	

* Because the X-ray structure of $[((CH_2)Me_2Si)_2N]_2Sn$ **2** has not been reported, the structural parameters of the loosely coordinated molecule of **2** found in $(\{[(CH_2)Me_2Si]_2N\}_2Sn)_3 \cdot CS_2$ **5** (vide supra) have been used as a comparison.

solution was cooled to −20 °C overnight. Green crystals of **5** were obtained (1.59 g, yield 99%, mp 98 °C). ^{1}H NMR (250 MHz, C_6D_6) δ 0.83 (s, 16 H, CH_2), 0.30 (s, 24 H, $Si(CH_3)_2$) ppm. $^{13}C\{^1H\}$ NMR (63 MHz, C_6D_6) δ 11.4 (s, CH_2), 3.9 (s, CH_3), S=*C*=S not observed. $^{119}Sn\{^1H\}$ (93 MHz, C_6D_6) δ 363 (broad), 83.5 (s), 18.0 (s) ppm. IR (Nujol): ν = 1523 (w), 869 (s). Elemental analyses for this compound consistently gave low values for C,H,N, even after multiple crystallizations and very sharp melting points; these low values may be due to silicon interference. Anal. Calcd for $C_{37}H_{96}N_6S_2Si_{12}Sn_3$ (M_w = 1382.47): C, 32.14; H, 7.01; N 6.08; S, 4.62. Found: C, 26.65; H, 6.08; N, 4.99; S, 4.52.

X-ray Crystallography. A single crystal of **3**, **4**, or **5** was coated with oil and mounted on a CryoLoop that had previously been attached using epoxy to a metallic pin. All measurements were made on a Bruker X8 Apex2 CCD-based X-ray diffractometer equipped with an Oxford Cryostream 700 low temperature device and normal focus Mo-target X-ray tube (λ = 0.71073 Å) operated at 1500 W power (50 kV, 30 mA). Data were collected at the temperatures indicated in Table 2 with the detector at a distance of 5.00 cm from the crystal.

Data collection and processing were done using the Bruker APEX2 software suite.[45] Structure solution was done with the SHELX suite of software.[46] Compounds **3** and **5** were solved by direct methods, and compound **4** was solved by Patterson methods, with the remaining atoms located in subsequent Fourier refinements. Non-hydrogen atoms were refined anisotropically, while hydrogen atoms were placed in geometrically calculated positions using a riding model. In compound **5**, C53, C54, and C55 were each disordered over two sites. They were modeled at 50% occupancy with equal anisotropic displacement parameters for each site. The disordered Si−C and C−C bond lengths were set at 1.87 and 1.52 Å, respectively. A summary of X-ray data can be found in Table 1.

Crystallographic data for the structures reported in this paper have been deposited with the Cambridge Crystallographic Data Centre as supplementary publications, nos. CCDC 714514 (**3**), 664586 (**4**), and 789678 (**5**). Copies of the data can be obtained free of charge on application to CCDC, 12 Union Road, Cambridge CB2 1EZ, U.K. (fax: (+44)1223−336−033; e-mail: deposit@ccdc.cam.ac.uk; www: http://www.ccdc.cam.ac.uk).

Acknowledgment. We thank Dr. Lev Zahkarov (University of Oregon) for help in modeling the disorder in **5**. Funding for this research was provided by NSF (CHE09-11110), the Sandia National Laboratories LDRD program (105932, 113486, and 149938) and the Natural Sciences and Engineering Research Council of Canada (postdoctoral fellowship to Dr. D. Dickie). The Bruker X8 X-ray diffractometer was purchased via an NSF CRIF:MU award to the University of New Mexico (CHE-0443580). Sandia is a multiprogram laboratory operated by Sandia Corporation, a Lockheed Martin Company, for the United States Department of Energy under Contract No. DE-AC04-94AL85000.

(45) *APEX2*; Bruker AXS, Inc.: Madison, WI, 2007.
(46) Sheldrick, G. M. *Acta Crystallogr.* **2008**, *A64*, 112–122.